Chemistry & Biology, Vol. 10, 645–654, July, 2003, ©2003 Elsevier Science Ltd. All rights reserved. DOI 10.1016/S1074-5521(03)00146-7

RNA LEGO: Magnesium-Dependent Formation of Specific RNA Assemblies through Kissing Interactions

Satoru Horiya,[1] Xianglan Li,[1] Gota Kawai,[2] Ryota Saito,[3] Akira Katoh,[3] Koh Kobayashi,[1] and Kazuo Harada[1,*]

[1]Department of Life Science
Tokyo Gakugei University
Koganei, Tokyo 184-8501
Japan

[2]Department of Industrial Chemistry
Chiba Institute of Technology
Narashino, Chiba 275-0016
Japan

[3]Department of Applied Chemistry
Faculty of Engineering
Seikei University
Musashino, Tokyo 180-8633
Japan

Summary

The high affinity and specificity of nucleic acid base complementarity has been proven to be a powerful method for constructing specific molecular assemblies. On the other hand, recent structural studies of RNA have revealed the wide range of tertiary interactions utilized in RNA folding, which may potentially be used as tools for the design of specific macromolecular assemblies. Here, RNA building blocks containing two hairpin loops, based on the dimerization initiation site (DIS) of HIV RNA, connected by a short linker were used to construct large RNA assemblies through hairpin loop-loop ("kissing") interactions. We show that specific linear and circular assemblies can be constructed in a magnesium-dependent manner using several non-self-complementary loop-loop interactions designed in this study. These results show that the use of RNA tertiary interactions may broaden the reportoire of nucleic acid-based nanostructures.

Introduction

Base-pairing interactions observed in nucleic acids, by virtue of their simplicity, have received considerable interest as a tool for creating specific macromolecular structures. In particular, DNA has been the material of choice for the construction of novel topologies [1, 2], in the design of molecular devices [3–6], and for application in molecular computation [7–9]. The assembly of such DNA structures has been carried out for the most part by Watson-Crick base pairing; however, noncanonical base-pairing schemes have also been utilized [6].

Recent progress in the understanding of RNA structure and folding has revealed a range of secondary and tertiary interactions, unique to RNA in biological systems [10–13], that may potentially be used in the construction of RNA-based assemblies. In a pioneering work by Jaeger and Leontis, a tetraloop-internal loop interaction has been used to construct dimeric and one-dimensional RNA structures [14–16], thereby expanding the utility of nucleic acids in the construction of nanomolecular structures.

The hairpin loop-loop interaction, or "kissing" interaction, is an interaction that has been found in antisense RNA control [17, 18], in the dimerization of retroviral genomic RNA [19–21], and in the folding of ribozymes [22–24]. The specificity of the kissing interaction is dictated by five to seven complementary base pairs between the two hairpin loops, while stacking interactions by surrounding bases provide stability to the interaction. Such kissing interactions have been shown to be 10^2–10^4 times more stable than the corresponding loop-linear interactions, as in the case of tRNAs and their complementary codons, which are more stable than the linear-linear interaction between complementary single-stranded regions [25], making loop-loop interactions sufficiently stable for constructing RNA assemblies.

The dimerization of the genomic RNA of the human immunodeficiency virus (HIV) is believed to occur first by a kissing interaction at a region termed the dimerization initiation site (DIS) and then by isomerization to a thermodynamically stable "tight" dimer [19, 26]. The nine-nucleotide DIS loop contains a self-complementary hexanucleotide (5′-GCGCGC-3′ in subtype B) flanked by purine residues that are thought to be important in stabilizing the kissing complex through noncanonical base-pairing and stacking interactions [27–30]. In vitro selection of loop variants capable of kissing complex formation has shown that the specificity of the interaction appears to be determined by base complementarity, so that the repertoire of loop-loop interactions that can be exploited for molecular assembly is potentially large [31]. In addition, the stability of the kissing interaction is highly dependent on magnesium concentration [19, 32], as with other known kissing complexes, suggesting that magnesium can be used as a switch for the assembly and disassembly of the RNA structures.

In this study, we have prepared RNA building blocks containing two hairpin loops based on the DIS connected by a two-nucleotide linker and studied the ability of these RNA building blocks to form linear and circular RNA assemblies (Figure 1A). We have shown by polyacrylamide gel electrophoresis that large RNA assemblies can be formed with the kissing interaction and that the formation of linear and circular arrangements of RNA building blocks is possible using non-self-complementary loop-loop pairs designed in this study. We also show by CD spectrometry that the RNA structures constructed in this way can be assembled and disassembled in a magnesium-dependent manner by adjusting the strength of the loop-loop interaction in a process we refer to as "RNA LEGO."

Results

Formation of Large RNA Assemblies through Loop-Loop (Kissing) Interactions

First, the assembly of the 56-mer RNA substrates **1–5** (Figure 1B) that contain two hairpin loops connected by

*Correspondence: harada@u-gakugei.ac.jp

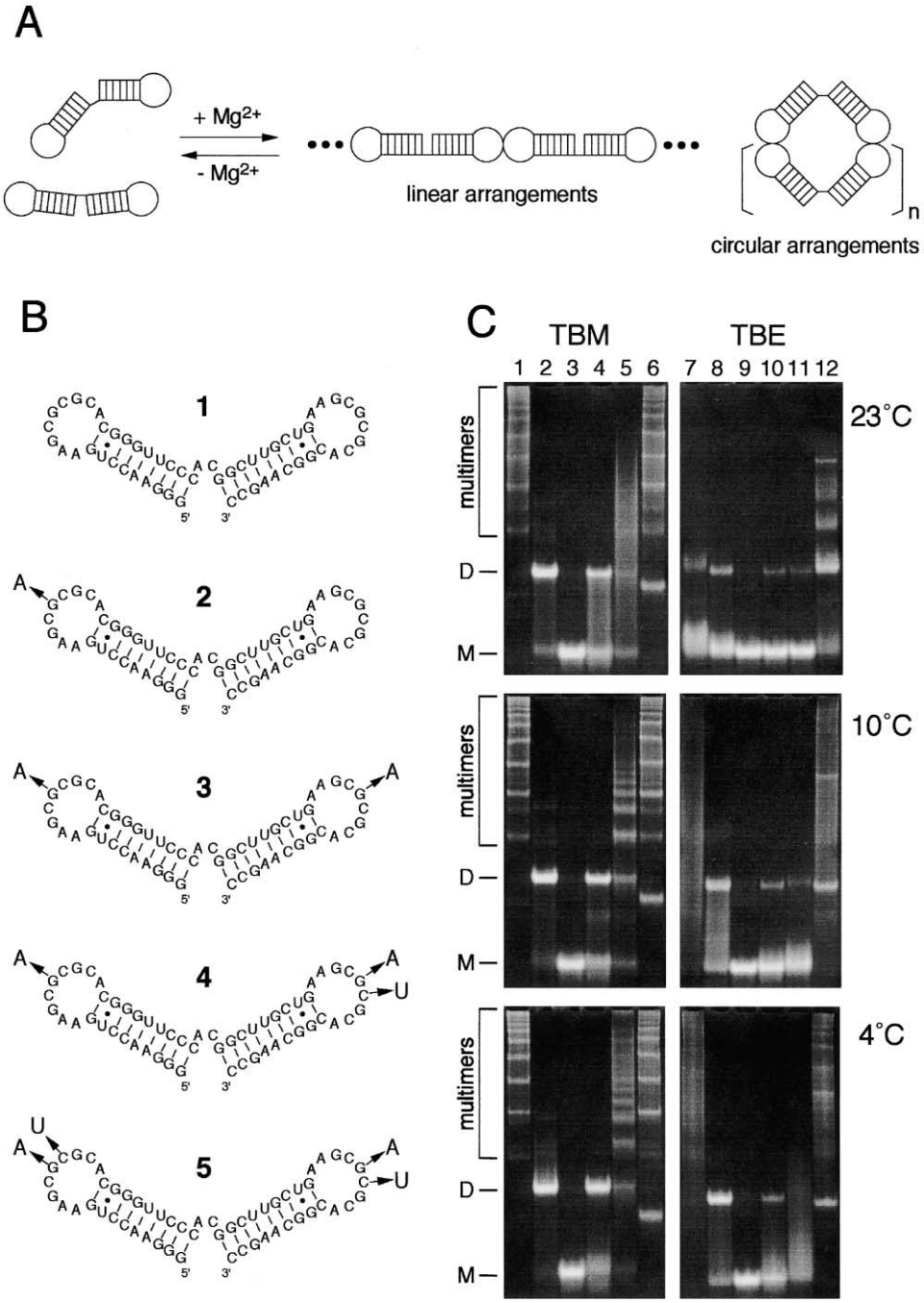

Figure 1. The Formation of RNA Assemblies with RNA Building Blocks **1–5**

(A) Scheme for the magnesium-dependent assembly of RNA building blocks.

(B) Secondary structure of RNA building blocks **1–5**.

(C) Analysis of the assembly of RNA building blocks (18 pmoles per lane) on TBM (0.1 mM Mg^{2+}) and TBE (no Mg^{2+}) gels at room temperature (23°C), 10°C, and 4°C. Lanes 1 and 7, substrate **1**; lanes 2 and 8, **2**; lanes 3 and 9, **3**; lanes 4 and 10, **4**; lanes 5 and 11, **5**; lanes 6 and 12, **1** (slow-cooled).

a two-nucleotide linker were studied. Each hairpin loop consisted of a nine-base pair stem and a loop sequence based on the self-complementary HIV dimerization initiation site (DIS) loop sequence (AAGCGCGCA; the self-complementary region is underlined). RNA substrates were heat denatured and quick-cooled, unless otherwise noted, to ensure the formation of the hairpin loop structures and analyzed by polyacrylamide gel electrophoresis (PAGE) on Tris-borate (TB) gels containing 0.1 mM magnesium (TBM gels) and gels lacking magnesium, but containing 2 mM EDTA (TBE gels), at several temperatures (Figure 1C). Low-gel mobility products,

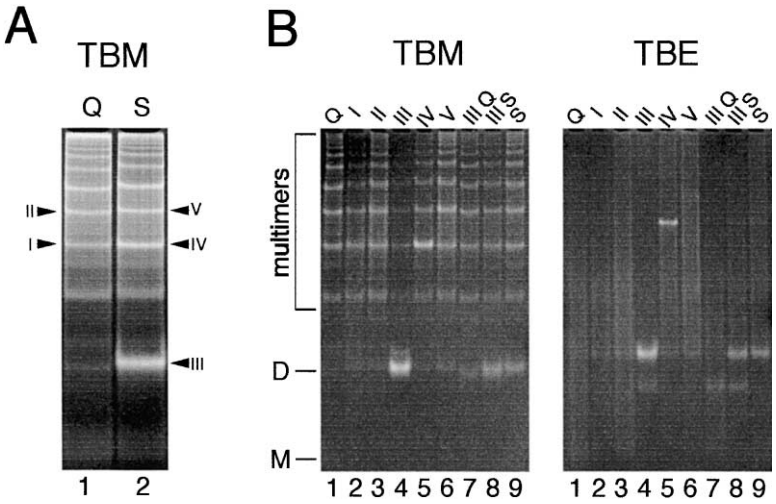

Figure 2. Reanalysis of Low-Mobility RNA Bands Excised from Polyacrylamide Gels

(A) TBM gel analysis of quick-cooled (Q) and slow-cooled (S) solutions of **1** at 10°C. RNA from bands I–V were eluted from the polyacrylamide gel.

(B) TBM and TBE gel analysis of RNA (4.5 pmoles per lane) from bands I–V excised from a TBM gel in (A) at 10°C. Lane 1, **1** (quick-cooled) (Q); lane 2, band I; lane 3, band II; lane 4, band III; lane 5, band IV; lane 6, band V; lane 7, band III (heated and quick-cooled); lane 8, band III (heated and slow-cooled); lane 9, **1** (heated and slow-cooled) (S).

most likely circular assemblies, were observed for RNA substrate **1** on TBM gels (Figure 1C, lane 1). On the other hand, on TBE gels, only small amounts of low-mobility products, which appear to decrease upon electrophoresis at higher temperature, were observed (Figure 1C, lane 7). This suggested that the majority of low-mobility products were associated through loop-loop interactions, since the rather weak DIS loop-loop complex has been shown to dissociate upon electrophoresis on TBE gels but is stabilized in the presence of magnesium on TBM gels [19, 32]. This is supported by the fact that the low-mobility bands are well defined on gels run at lower temperatures (10°C and 4°C) compared to gels run at room temperature (23°C) (Figure 1C, lane 1), which presumably reflects the stabilization of the rather weak kissing interactions at low temperatures. The smearing of bands observed in the TBE gel (Figure 1C, lane 7), particularly at low temperatures, was thought to be due to such dissociation of the loop-loop interaction during electrophoresis. By contrast, when **1** was heated and slow-cooled prior to gel electrophoresis, dimeric and larger products were observed on both TBM and TBE gels, indicating that a portion of the RNA building blocks were not kissing but were extensively base paired (Figure 1C, lanes 6 and 12) because slow-cooling leads to intermolecular base-paired structures that are stable in the absence of magnesium.

In order to provide evidence that the low-mobility products observed for **1** were indeed assembled via kissing interactions, we analyzed substrates **2** and **3**, which contain loop mutations that disrupt kissing complexes, as well as substrates **4** and **5**, which contain mutations that complement these loop mutations and restore kissing complex formation. RNAs with a G to A mutation in one (**2**) or both of the loops (**3**) resulted in the formation of a dimeric and a monomeric arrangement, respectively, on the basis of gel mobility (Figure 1C, lanes 2 and 3). Furthermore, substrates that contain additional single or double C to U mutations that complement the G to A mutations (**4** and **5**) were found to restore formation of dimeric or larger RNA assemblies (Figure 1C, lanes 4 and 5).

To further show that the low-mobility products observed on TBM gels were held together by kissing interactions, we excised specific low-mobility bands (I–V) formed upon quick-cooling (Q) and slow-cooling (S) of substrate **1** from a TBM gel (Figure 2A), and the RNA was extracted from the gel slices and rerun on TBM and TBE gels (Figure 2B). Upon rerunning RNA from bands I and II, which were formed from quick-cooled samples, we observed reequilibration of the RNA building blocks to form a series of bands with differing gel mobility on a TBM gel (Figure 2B, lanes 2 and 3), while these bands could not be observed on a TBE gel (Figure 2B, lanes 2 and 3). On the other hand, upon rerunning RNA from bands III and IV, which were formed from slow-cooled samples, we observed defined bands with a mobility similar to that of the excised band on both TBM and TBE gels (Figure 2B, lanes 4 and 5), indicating that these RNA products were extensively base paired. In addition, when the RNA from band III was heat denatured and then quick- or slow-cooled, a series of low-mobility bands was again observed (Figure 2B, lanes 7 and 8).

Disruption of the Formation of RNA Assemblies with Competitor Substrates

Since it appeared likely that the low-mobility bands observed for substrate **1** were circular arrangements, a competition experiment where substrate **2** was added to disrupt the energetically weak kissing interaction in the circular complexes of substrate **1** was carried out. After addition of increasing amounts of **2** to a preformed solution of **1** and incubation for 30 min at 37°C, the accumulation of a series of new high-mobility bands, presumably corresponding to linear arrangements, was observed (Figure 3A, lanes 2–8). On the other hand, addition of substrate **3**, which is incapable of kissing with substrate **1**, did not disrupt the formation of high-order assemblies (Figure 3A, lane 9). Next, upon addition of magnesium (to 1 or 5 mM) prior to the addition of the competitor, the RNA assemblies were converted to a competitor-resistant form, as shown in Figure 3B. This result shows that the conformation of the RNA assemblies can be "locked" in position by addition of magnesium.

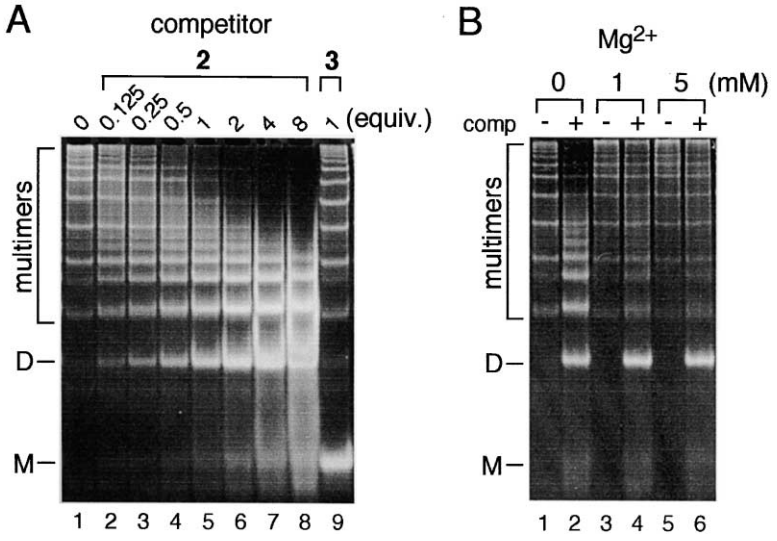

Figure 3. Disruption of the Formation of RNA Assemblies by the Addition of Competitor Substrates

(A) Competitor RNA (**2** or **3**) in 1× PN buffer was added to a premixed solution of **1** (18 pmoles) in 1× PN buffer, incubated at 37°C for 30 min, and analyzed on a TBM gel at 10°C. Lane 1, **1** alone; lanes 2–8, **1** plus competitor **2** in the amounts indicated; lane 9, **1** plus competitor **3**.

(B) Mg^{2+} was added to solutions of competitor RNA (**2**; 9 pmoles) and **1** (9 pmoles) that had been individually heated and quick-cooled in the usual manner. The two solutions were mixed, incubated for 30 min at 31°C, and analyzed on a TBM gel at 10°C.

The Design of Non-Self-Complementary Loop-Loop Complexes

In order to construct specific linear and circular arrangements of RNA building blocks through loop-loop interactions, we needed to design pairs of non-self-complementary loop sequences. We therefore prepared nine pairs of RNA hairpin loops containing non-self-complementary loop sequences (Figure 4A, A1/A2–I1/I2), which included two previously reported RNA pairs (A1/A2 and G1/G2) [31], and determined their affinity using a gel mobility shift assay at 23°C and 4°C (Figure 4A). The stability of the pairs of loop sequences observed by the gel shift assay corresponded roughly to the thermodynamic stability calculated with the expanded nearest-neighbor parameters determined by Turner and coworkers for the formation of RNA duplexes (Figure 4B) [33]. Next, the six pairs of RNA loop sequences showing the highest affinity (loop sequences A1/A2–F1/F2) were tested for specificity of binding to their cognate loop sequences by analyzing all 78 combinations of RNA

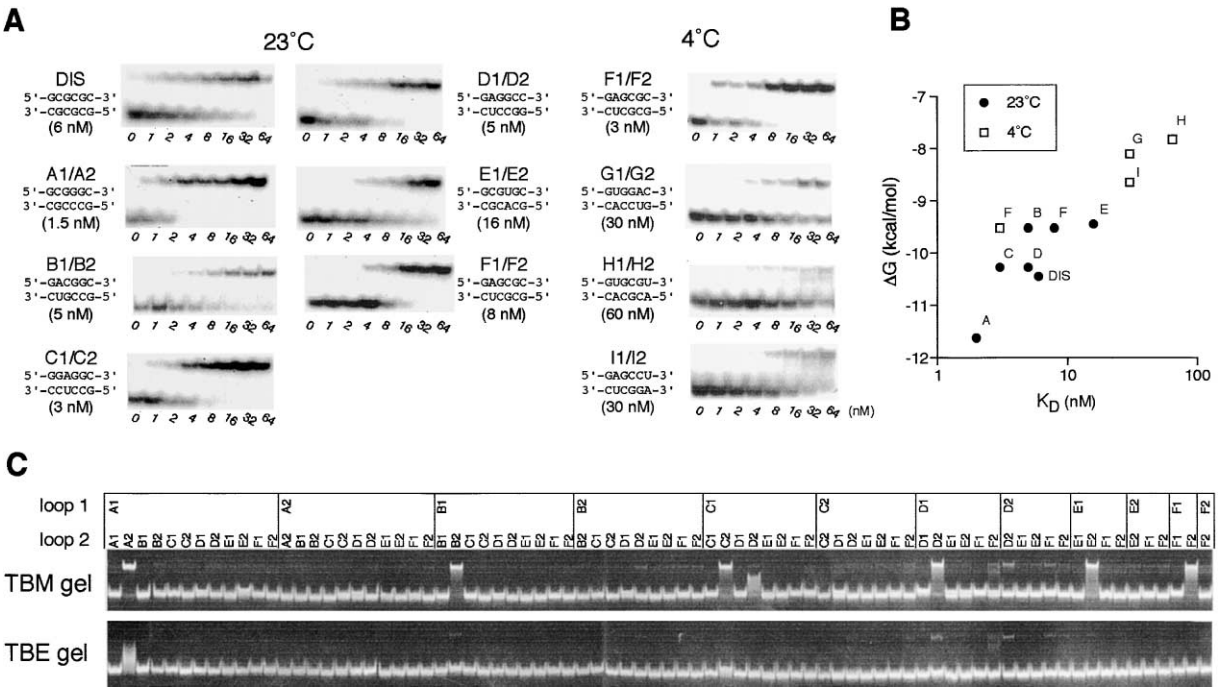

Figure 4. The Design of Novel Non-Self-Complementary Kissing Complexes Based on the DIS Loop Sequence

(A) Gel shift analysis of kissing complex formation of 27-mer hairpin loop RNAs on TBM gels at 23°C and 4°C.

(B) Relationship between relative K_Ds and calculated thermodynamic stability (ΔG°_{37}) of kissing complexes.

(C) Analysis of the specificity of kissing complex formation by loop sequences A–F by mixing equimolar amounts of all 78 combinations of RNA hairpins on TBM and TBE gels.

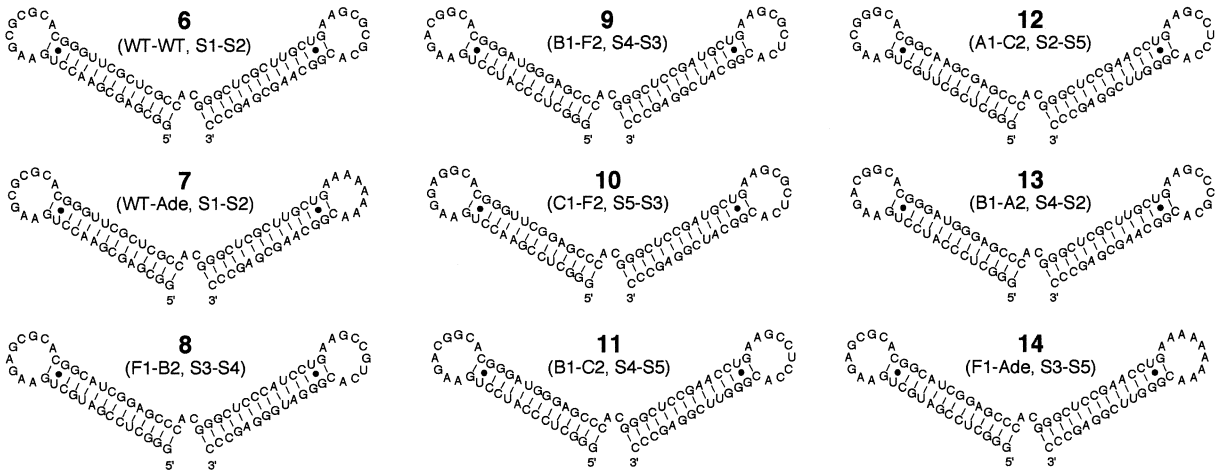

Figure 5. The Secondary Structures of RNA Building Blocks **6–14**

In parenthesis, the combination of 5′- and 3′-loop sequences used (WT DIS, A1-F2, or Ade [a hexaadenylate sequence]) and the combination of 5′- and 3′-stem sequences used (S1–S5) are indicated.

pairs by PAGE on TBM and TBE gels, as shown in Figure 4C. While some promiscuous behavior by loop sequences D1 and D2 was observed, as indicated by the small amount of dimeric species observed in the TBM gel (Figure 4C), the remaining five pairs (A, B, C, E, and F) were found to be highly specific for their complementary partners.

Construction of Specific Linear and Circular Arrangements

RNA building blocks **6–14** consisting of two hairpin loops connected by a two nt linker, as in the case of RNAs **1–5**, but with 14 base pair stems, were prepared. The longer stem was expected to reduce potential isomerization to the stable extended dimer (Figure 5). Substrates **6–14** were mixed in specific combinations, heated, quick-cooled, incubated at 37°C in PN buffer, and analyzed by PAGE on TBM and TBE gels (Figures 6A and 6B). As expected, defined bands could not be observed on TBE gels (Figure 6B), while specific low-mobility bands were observed on the TBM gel as described below (Figure 6A).

RNA building block **6** containing the self-complementary DIS hexanucleotide sequence in both loops formed a series of circular arrangements, as shown in lanes 1 and 19 (Figure 6A). When substrate **7** containing the DIS hexanucleotide in one loop and a hexaadenylate in the other loop was added to this solution of **6**, opening of the circular arrangements to form what were assumed to be a series of linear arrangements was observed (lanes 2 and 18). RNA building blocks **8–14** contained various combinations of the non-self-complementary loop sequences A1–F2 (Figure 5) and were designed to assemble into the linear and circular structures shown in Figure 6C. The specific formation of monomer (M), linear dimer (l-D), linear trimer (l-Tri), and linear tetramer (l-Tet) is shown in lanes 3, 4, 10, and 14, respectively, and corresponded with the series of bands observed in lanes 2 and 18. The specific formation of circular dimer (c-D), circular trimer (c-Tri), and circular tetramer (c-Tet) can be observed in lanes 5, 11, and 15, respectively, and again corresponded to the series of bands observed in lanes 1 and 19. Furthermore, as would be expected, formation of circular dimer (c-D) was accompanied by the formation of what appeared to be circular tetramer (c-Tet) and circular hexamer (c-Hex) (lane 5). Similarly, formation of circular trimer (c-Tri) and circular tetramer (c-Tet) were accompanied by the formation of circular hexamer (c-Hex) and circular octamer (c-Oct), respectively, as well as even-higher-order assemblies (lanes 11 and 15). An experiment where RNA substrates were individually heated, quick-cooled, and then mixed at specific ratios resulted in an identical distribution of circular products to that when the mixture of RNAs was heated and quick-cooled (lanes 5 and 6).

The formation of specific circular arrangements, as shown in Figure 6A (lanes 5, 11, and 15), was further supported by experiments where **14** was added as a competitor to disrupt formation of the circular structures. Upon addition of increasing amounts of competitor RNA **14** to the solution containing the preformed c-D, which also contains a considerable amount of c-Tet and c-Hex, a decrease in the amount of c-D (and c-Tet and c-Hex) was accompanied by an increase in the amount of linear trimer (l-Tri) (lanes 7 and 8). Similar treatment of solutions containing the preformed circular trimer (c-Tri) and circular tetramer (c-Tet) with competitor **14** led to the formation of linear tetramer (l-Tet) and linear pentamer (l-Pent), respectively (lanes 12, 13, 16, and 17). An experiment where the RNA substrates including the competitor (**14**) were mixed prior to heating and quick-cooling resulted in an identical distribution of products to that when the competitor was added to the preformed circular dimer (lanes 8 and 9).

Observation of the Magnesium-Dependent Assembly of RNA Building Blocks by CD

Since the stability of the loop-loop interaction is highly dependent on magnesium concentration, we attempted the observation of the magnesium-dependent assembly

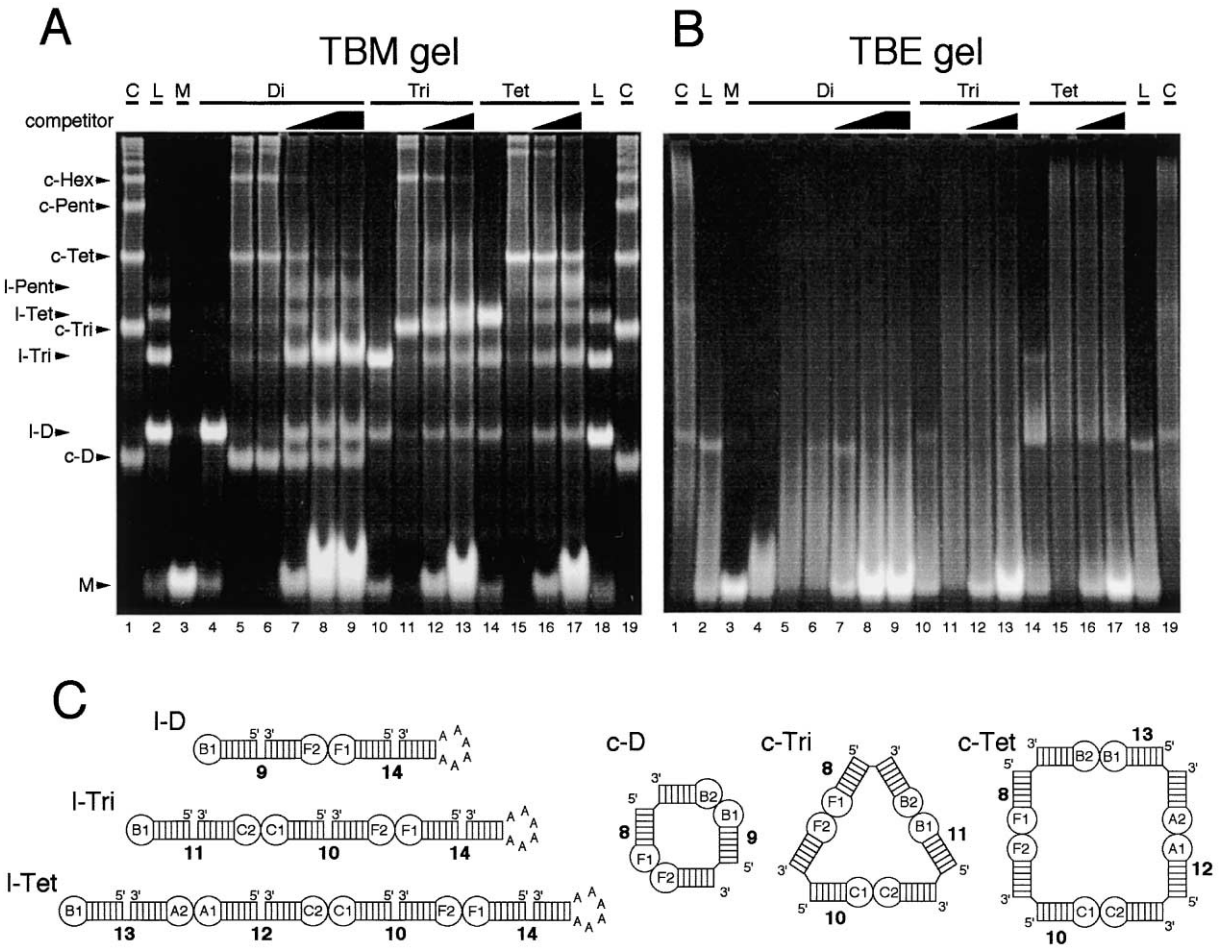

Figure 6. The Formation of Specific Arrangements of RNA Building Blocks

(A) TBM (plus Mg^{2+}) gel analysis of RNA assemblies at 10°C. The total amount of RNA was 12 pmoles with the exception of the competition experiments. Lane 1, **6**; lane 2, **6** and **7** (1:5); lane 3, **9**; lane 4, **9** and **14** (1:1); lane 5, **8** and **9** (individually annealed and mixed 1:1); lane 6, **8** and **9** (1:1); lane 7, **8** and **9** (1:1) plus **14** (molecular equivalents); lane 8, **8** and **9** (1:1) plus **14** (5 molecular equivalents); lane 9, **8**, **9**, and **14** (1:1:5); lane 10, **10**, **11**, and **14** (1:1:1); lane 11, **8**, **10**, and **11** (1:1:1); lane 12, **8**, **10**, and **11** (1:1:1) plus **14** (molecular equivalents); lane 13, **8**, **10**, and **11** (1:1:1) plus **14** (5 molecular equivalents); lane 14, **10**, **12**, **13**, and **14** (1:1:1:1); lane 15, **8**, **10**, **12**, and **13** (1:1:1:1); lane 16, **8**, **10**, **12**, and **13** (1:1:1:1) plus **14** (molecular equivalents); lane 17, **8**, **10**, **12**, and **13** (1:1:1:1) plus **14** (5 molecular equivalents); lane 18, same as lane 2; lane 19, same as lane 1.

(B) TBE gel analysis of RNA assemblies as described in (A) at 10°C.

(C) Proposed structures of the designed circular dimer (c-Di), circular trimer (c-Tri), circular tetramer (c-Tet), linear dimer (l-Di), linear trimer (l-Tri), and linear tetramer (l-Tet).

of RNA building blocks by CD spectrometry, which is sensitive to changes in RNA structure. Upon addition of magnesium to a solution of RNA substrate **1** at 25°C (Figure 7A, closed diamonds), a small increase in the CD band centered at ~260 nm was observed (Figure 7A, open circles). On the other hand, upon heating the solution of **1**, a considerable increase in the CD band centered at ~280 nm was observed (Figure 7A, plus signs). The latter change was assumed to be due mostly to the dissociation of the kissing complexes, since the WT DIS hairpin loop has been shown to "kiss" even in the absence of magnesium [34].

From this result, it was anticipated that the magnesium-dependent formation of RNA assemblies could be observed by lowering the affinity of the loop-loop complexes. Indeed, upon addition of magnesium (1 mM) to a solution of **5** (Figure 7B, closed diamonds), which possesses a GCAUGC in the loop, with an estimated 50-fold-lower affinity compared to the WT DIS loop (on the basis of the calculated thermodynamic stability), the increase in the CD band centered at ~260 nm was accompanied by a decrease of the CD band at 270–290 nm (Figure 7B, open circles). Addition of EDTA to this solution resulted in a small decrease in the CD band at 250–270 nm, while the magnesium-induced decrease in the CD band at 270–290 nm persisted. However, by further heating this solution to 45°C and returning the temperature to 25°C, the CD band at 270–290 nm returned to the original state of the free RNA (Figure 7B, plus signs). We believe that the increase in the CD band at 250–270 nm represents, for the most part, a nonspecific RNA conformational change, while the CD band

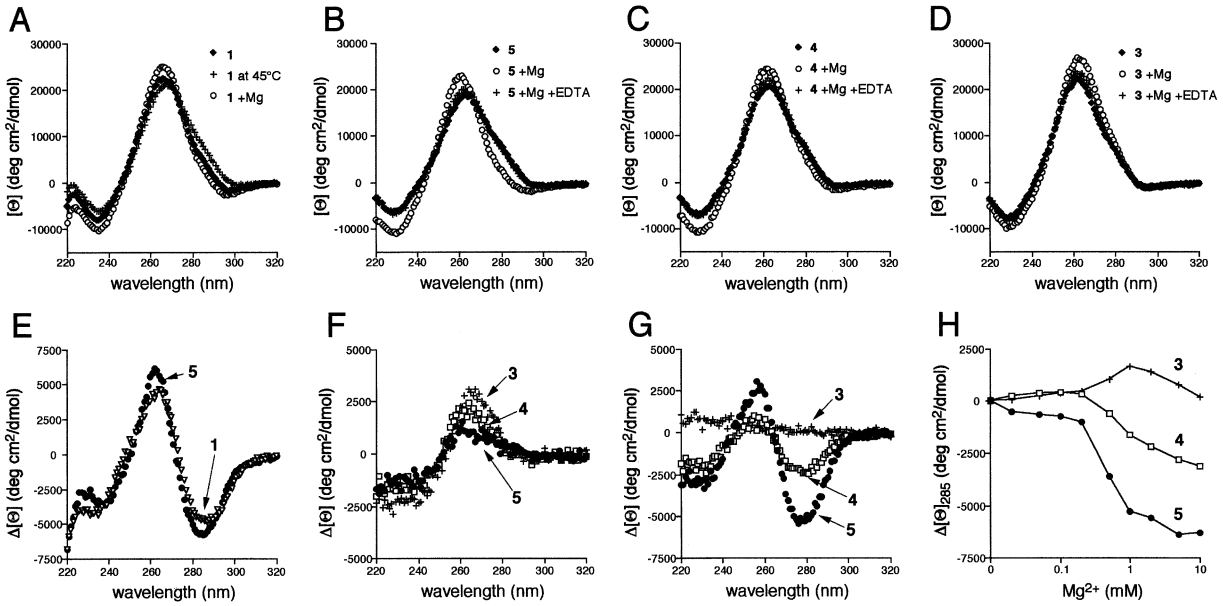

Figure 7. CD Spectra of Substrates **1**, **5**, **4**, and **3** (1.6 μM) in 10 mM Phosphate Buffer (pH 7.0) at 25°C

(A) CD spectra of **1** (WT) (closed diamonds) after addition of Mg^{2+} to 1 mM (open circles) and heating to 45°C (plus signs).

(B–D) CD spectra of **5**, **4**, and **3** (closed diamonds) after addition of $MgCl_2$ to 1 mM (open circles), further addition of EDTA to 1 mM, heating to 45°C, and cooling to 25°C (plus signs).

(E) A comparison of the CD change induced by heat and Mg^{2+} treatment of **1** (open triangles) ([A], open circles minus plus signs) and upon addition of Mg^{2+} to **5** (closed circles) ([B], open circles minus closed diamonds).

(F) Difference spectra of **3** (plus signs), **4** (open squares), and **5** (closed circles) before and after addition of EDTA.

(G) Difference spectra of **3** (plus signs), **4** (open squares), and **5** (closed circles) before and after 45°C treatment.

(H) Change in molar ellipticity (Θ) at 285 nm upon magnesium titration of substrates **3** (plus signs), **4** (open squares), and **5** (closed circles).

at 270–290 nm represents the conformational change induced by kissing complex formation. A difference spectra of the CD change induced by heating and adding Mg^{2+} to a solution of **1** (open triangles) and by addition of magnesium to **5** (closed circles) was found to coincide, as shown in Figure 7E, indicating that the formation of the kissing complex can be regulated by Mg^{2+} and by heat.

Similar experiments with **4** (Figure 7C), which can only kiss through one loop, and **3** (Figure 7D), which is incapable of kissing, showed that the decrease in the CD band at 270–290 nm corresponded to the number of potential kissing complexes (Figures 7C and 7D). A difference spectra of the CD change induced by the kissing interaction is shown in Figure 7G, while the nonspecific CD change induced by magnesium is shown in Figure 7F. A magnesium titration curve of the change at 285 nm is shown in Figure 7H, where the CD change observed for **5** was twice that of **4**, corresponding to the number of potential loop-loop interactions.

Discussion

Jaeger and Leontis have previously demonstrated the use of RNA tertiary interactions in the design of large macromolecular RNA assemblies. In this case, the GAAA tetraloop/11 nt receptor interaction was used to form dimeric and one-dimensional RNA assemblies [15, 16]. We have utilized a similar strategy using the kissing interaction of the DIS, the dimerization site of HIV RNA, for the construction-specific linear and circular RNA arrangements. The kissing interaction used in this study is distinct from the GAAA tetraloop/11 nt receptor interaction used in the work of Jaeger and Leontis, in that the former is mediated primarily by Watson-Crick base pairing of loop nucleotides, while the latter consists of non-Watson-Crick pairing. Thus, the specificity of the kissing interaction of the DIS could be readily switched by substitution to an alternative complementary loop sequence, as was suggested from in vitro selection of DIS variants performed by Marquet and coworkers [31]. When the affinity and specificity of several non-self-complementary loop-loop pairs was analyzed, the stability of kissing complexes determined by gel shift analysis was found to roughly correlate with the stability of the corresponding hexanucleotide duplexes calculated by thermodynamic parameters determined by Turner and coworkers (Figure 4B) [33]. This result is in contrast with the stabilities observed for kissing complexes based on the *E. coli* RNA I and RNA II interaction, where the melting temperatures of kissing complexes do not correlate with the calculated stability of the corresponding heptanucleotide duplexes [35]. Thus, the sequence dependence of kissing complex stability appears to differ depending on the context of the loop. The ability to predict the stability of the kissing complex in the DIS framework enables one to readily adjust the strength of the interaction to one's purpose, therefore making it an attractive tool for the assembly of RNA building blocks.

Since the kissing interaction is known to be stabilized

in the presence of magnesium ion, it was anticipated that the assembly and the disassembly of the RNA building blocks could be controlled in a manner similar to the way that protein subunits reversibly assemble into functional quarternary structures [36]. Indeed, the stabilization of the RNA assemblies of **1** by magnesium ion could be observed as the presence of defined RNA bands on TBM gels (Figure 1C, lane 1) as compared to the absence of RNA bands on TBE gels (Figure 1C, lane 7). However, **1**, which possesses the DIS loop, was shown to be able to form a kissing complex in the absence of magnesium at room temperature by CD (Figure 7A). Apparently, in the absence of magnesium, the weakly associated kissing complexes of **1** dissociate during PAGE, as indicated by the smearing observed on TBE gels (Figure 1C, lane 7). On the other hand, since the kissing complex formed for **1** could be dissociated by heating to 45°C (Figure 7A), it was expected that the assembly of RNA building blocks could be made to be magnesium dependent by lowering the stability of the loop-loop interaction. As expected, by substituting the DIS loop sequence (GCGCGC) with a weakly binding loop sequence (the GCAUGC of **5**), kissing complex formation was abolished in the absence of magnesium but was induced by the addition of magnesium (to 1 mM), as observed by CD.

Significance

A number of characteristics of the kissing complex make it potentially useful for the design of nucleic acid-based nanostructures. First, the ability to assemble or disassemble the RNA building blocks in a magnesium-dependent manner as shown in this study may be used as a switch for assembling RNA nanostructures and in bringing functional groups into close proximity. Second, kissing complexes identified in biological systems often isomerize to a more thermodynamically stable structure and, by doing so, act as functional switches [17, 18]. In the case of the kissing complex formed by the HIV DIS, the isomerization is facilitated by the RNA chaperone activity of NCp7 protein [37] or in vitro by heat treatment [19–21, 32]. Therefore, the protein- or thermally-induced isomerization of RNA assemblies may be used as a functional switch. RNA structures constructed in this way may also act as scaffolds for the construction of complex molecular assemblies, for example, by the introduction of protein binding sites. While RNA-based assemblies such as those presented in the present study may not find broad applications because of their enzymatic and chemical instability, they may provide a starting point for the design of novel functional DNA-based assemblies, since unique structures and functions identified from studies of RNA have often been shown to occur with single-stranded DNA (ssDNA) [38]. In fact, a DNA version of the self-complementary DIS has recently been shown to form a loop-loop complex, although the details of the interaction are somewhat different [39]. In addition to the possible importance of such an approach in constructing specific nanomolecular structures, we believe that the results are interesting from a structural perspective, in that they may provide insights into the way in which large RNA-based structures are formed.

Experimental Procedures

Materials

RNA substrates were transcribed in vitro with T7 RNA polymerase and DNA templates that had been prepared from synthetic DNAs. DNA templates for 56-mer (Figure 1B) and 27-mer (5′-GGCUUGCU GAANNNNNNACGGCAAGCC-3′, where NNNNNN was one of the 19 hexanucleotide sequences [DIS and A1-I2] shown in Figure 4A) RNA substrates were prepared by annealing the synthetic single-stranded DNA templates and an 18-mer T7 promoter DNA (5′-GTAA TACGACTCACTATA-3′). DNA templates for 76-mer RNA substrates (Figure 5) were prepared by annealing two oligonucleotides complementary at the 3′-end and by second strand synthesis with Taq polymerase.

Native Polyacrylamide Gel Electrophoresis (PAGE) Analysis of RNA Substrates

Native PAGE analysis of the assembly of the 56-mer RNAs **1–5**, 76-mer RNAs **6–14**, and 27-mer RNAs was performed by the following general protocol, unless otherwise noted. RNA substrate(s) (**1–5**, 36 pmoles; **6–14**, a total of 24 pmoles per experiment; 27-mer RNA, 80 pmoles) in H_2O (typically 6 μl for **1–14** and 8 μl for the 27-mers) were heated at 95°C for 5 min and immediately cooled on ice. To this solution, we added 4× PN buffer (2× for 27-mer RNAs) to give a final concentration of 10 mM sodium phosphate (pH 7.0) and 50 mM NaCl (1× PN buffer) and incubated it at 37°C (room temperature for 27-mers) for 30 min [32]. In the case of slow-cooled samples, the RNA (36 pmoles) in 1× PN buffer (8 μl) was heated at 95°C for 5 min and slowly cooled to room temperature over a period of up to 2 hr. To these solutions, we added one-fourth the volume (an equal volume for 27-mers) of a loading buffer containing glycerol, and the solution was divided into two aliquots and analyzed separately by electrophoresis on nondenaturing 8% (15% for 27-mer RNAs) polyacrylamide gels (acrylamide/bisacrylamide ratio of 30:1 for **1–14** and 20:1 for 27-mer RNAs) in TBM-buffer (89 mM Tris, 89 mM borate, and 0.1 mM $MgCl_2$) and TBE-buffer (89 mM Tris, 89 mM borate, and 2 mM EDTA) at 4°C to room temperature (23°C). RNA bands were visualized by staining with ethidium bromide and irradiation with a UV transilluminator. When mixtures of multiple RNAs were analyzed, the RNAs were mixed prior to heating and quick-cooling, with the exception of the competition experiments, where a competitor RNA was added to the premixed RNA solutions, and where otherwise noted.

Excision and Reanalysis of RNA Assemblies with Low Electrophoretic Mobility

RNA substrate **1** (160 μl of a 4.5 μM solution) that had been quick-cooled or slow-cooled as described above was run on an 8% polyacrylamide/TBM gel. RNAs were excised from the gel, eluted from the gel slice, ethanol precipitated, and redissolved in H_2O. Six microliter 1.5 μM solutions of the isolated RNAs were mixed with 4× PN buffer (2 μl), incubated at 37°C for 30 min or quick- or slow-cooled, divided into two aliquots, and analyzed as described above on TBM and TBE gels.

Gel Shift Assays

Internally labeled 27-mer RNAs were transcribed in vitro with T7 RNA polymerase as previously described [40]. A 2 nM solution of the internally labeled RNA (A2–I2) (4 μl) was mixed with an equal volume of a 0–256 nM solution of the cold RNA (A1–I1), heated at 95°C for 5 min, and cooled immediately on ice. Eight microliters of 2× PN buffer was added to this solution, the mixture was incubated for 30 min at room temperature, one-forth the volume of a glycerol loading buffer was added, and the mixture was analyzed on TBM gels at room temperature and/or at 4°C.

Circular Dichroism (CD)

CD spectra were measured with an Aviv model 202 spectrometer. RNA samples (12 μM) in H_2O were heated at 95°C for 5 min and then immediately chilled on ice. To this solution, we added sodium phosphate buffer (pH 7.0) to a final concentration of 10 mM with a 2× solution. This solution was incubated for 30 min at 37°C, and the RNA concentration was adjusted to 1.6 μM with 10 mM phoshate buffer. Spectra were recorded with a 1 cm pathlength cuvette at 25°C, and the signal was averaged for 3 s at each wavelength. Mean molecular ellipticity was calculated per nucleotide of the RNA.

Acknowledgments

We thank an anonymous reviewer for many helpful suggestions. This research was supported by a Grant-in-Aid for Scientific Research on Priority Areas from the Ministry of Education, Culture, Sports, Science and Technology, Japan.

Received: April 28, 2003
Revised: May 30, 2003
Accepted: June 2, 2003
Published: July 18, 2003

References

1. Seeman, N.C. (1999). DNA engineering and its application to nanotechnology. Trends Biotechnol. *17*, 437–443.
2. Seeman, N.C., and Belcher, A.M. (2002). Emulating biology: building nanostructures from the bottom up. Proc. Natl. Acad. Sci. USA *99*, 6451–6455.
3. Mao, C., Sun, W., Shen, Z., and Seeman, N.C. (1999). A nanomechanical device based on the B-Z transition of DNA. Nature *397*, 144–146.
4. Yurke, B., Turberfield, A.J., Mills, A.P., Jr., Simmel, F.C., and Neumann, J.L. (2000). A DNA-fuelled molecular machine made of DNA. Nature *406*, 605–608.
5. Yan, H., Zhang, X., Shen, Z., and Seeman, N.C. (2002). A robust DNA mechanical device controlled by hybridization topology. Nature *415*, 62–65.
6. Venczel, E.A., and Sen, D. (1996). Synapsable DNA. J. Mol. Biol. *257*, 219–224.
7. Adleman, L.M. (1994). Molecular computation of solutions to combinatorial problems. Science *266*, 1021–1024.
8. Benenson, Y., Paz-Elizur, T., Adar, R., Keinan, E., Livneh, Z., and Shapiro, E. (2001). Programmable and autonomous computing machine made of biomolecules. Nature *414*, 430–434.
9. Mao, C., LaBean, T.H., Reif, J.H., and Seeman, N.C. (2000). Logical computation using algorithmic self-assembly of DNA triple-crossover molecules. Nature *407*, 493–496.
10. Burkard, M.E., Turner, D.H., and Tinoco, I., Jr. (1999). The interactions that shape RNA structure. In The RNA World, Second Edition, R.F. Gesteland, T.R. Cech, and J. F. Atkins, eds. (Plainview, NY: Cold Spring Harbor Laboratory Press), pp. 233–264.
11. Hermann, T., and Patel, D.J. (1999). Stitching together RNA tertiary architectures. J. Mol. Biol. *294*, 829–849.
12. Batey, R.T., Rambo, R.P., and Doudna, J.A. (1999). Tertiary motifs in RNA structure and folding. Angew. Chem. Int. Ed. Engl. *38*, 2326–2343.
13. Westhof, E., and Fritsch, V. (2000). RNA folding: beyond Watson-Crick pairs. Structure *8*, R55–R65.
14. Westhof, E., Masquida, B., and Jaeger, L. (1996). RNA tectonics: towards RNA design. Fold. Des. *1*, R78–R88.
15. Jaeger, L., and Leontis, N.B. (2000). Tecto-RNA: one-dimensional self-assembly through tertiary interactions. Angew. Chem. Int. Ed. *39*, 2521–2524.
16. Jaeger, L., Westhof, E., and Leontis, N.B. (2001). TectoRNA: modular assembly units for the construction of RNA nanoobjects. Nucleic Acids Res. *29*, 455–463.
17. Wagner, E.G.H., and Simons, R.W. (1994). Antisense RNA control in bacteria, phages, and plasmids. Annu. Rev. Microbiol. *48*, 713–742.
18. Eguchi, Y., Itoh, T., and Tomizawa, J.-i. (1991). Antisense RNA. Annu. Rev. Biochem. *60*, 631–652.
19. Laughrea, M., and Jette, L. (1996). Kissing-loop model of HIV-1 genome dimerization: HIV-1 RNAs can assume alternative dimeric forms, and all sequences upstream or downstream of hairpin 248–271 are dispensable for dimer formation. Biochemistry *35*, 1589–1598.
20. Paillart, J.-C., Skripkin, E., Ehresmann, B., Ehresmann, C., and Marquet, R. (1996). A loop-loop "kissing" complex is the essential part of the dimer linkage of genomic HIV-1 RNA. Proc. Natl. Acad. Sci. USA *93*, 5572–5577.
21. Muriaux, D., Fosse, P., and Paoletti, J. (1996). A kissing complex together with a stable dimer is involved in the HIV-1 Lai RNA dimerization process *in vitro*. Biochemistry *35*, 5075–5082.
22. Lehnert, V., Jaeger, L., Michel, F., and Westhof, E. (1996). New loop-loop tertiary interactions in self-splicing introns of subgroup IC and ID: a complete 3D model of the *Tetrahymena thermophila* ribozyme. Chem. Biol. *3*, 993–1009.
23. Ikawa, Y., Ohta, H., Shiraishi, H., and Inoue, T. (1997). Long-range interaction between the P2.1 and P9.1 peripheral domains of the *Tetrahymena* ribozyme. Nucleic Acids Res. *25*, 1761–1765.
24. Andersen, A.A., and Collins, R.A. (2001). Intramolecular secondary structure rearrangement by the kissing interaction of the *Neurospora* VS ribozyme. Proc. Natl. Acad. Sci. USA *98*, 7730–7735.
25. Zeiler, B.N., and Simons, R.W. (1998). Antisense RNA structure and function. In RNA Structure and Function, R.W. Simons and M. Grunberg-Manago, eds. (Plainview, NY: Cold Spring Harbor Laboratory Press), pp. 437–464.
26. Skripkin, E., Paillart, J.-C., Marquet, R., Ehresmann, B., and Ehresmann, C. (1994). Identification of the primary site of the human immunodeficiency virus type 1 RNA dimerization *in vitro*. Proc. Natl. Acad. Sci. USA *91*, 4945–4949.
27. Jossinet, F., Paillart, J.-C., Westhof, E., Hermann, T., Skripkin, E., Lodmell, J.S., Ehresmann, C., Ehresmann, B., and Marquet, R. (1999). Dimerization of HIV-1 genomic RNA of subtypes A and B: RNA loop structure and magnesium binding. RNA *5*, 1222–1234.
28. Dardel, F., Marquet, R., Ehresmann, C., Ehresmann, B., and Blanquet, S. (1998). Solution studies of the dimerization initiation site of HIV-1 genomic RNA. Nucleic Acids Res. *26*, 3567–3571.
29. Mujeeb, A., Clever, J.L., Billeci, T.M., James, T.L., and Parslow, T.G. (1998). Structure of the dimer initiation complex of HIV-1 genomic RNA. Nat. Struct. Biol. *5*, 432–436.
30. Ennifar, E., Walter, P., Ehresmann, B., Ehresmann, C., and Dumas, P. (2001). Crystal structures of coaxially stacked kissing complexes of the HIV-1 RNA dimerization initiation site. Nat. Struct. Biol. *8*, 1064–1068.
31. Lodmell, J.S., Ehresmann, C., Ehresmann, B., and Marquet, R. (2000). Convergence of natural and artificial evolution on an RNA loop-loop interaction: the HIV-1 dimerization initiation site. RNA *6*, 1267–1276.
32. Takahashi, K.-i., Baba, S., Chattopadhyay, P., Koyanagi, Y., Yamamoto, N., Takaku, H., and Kawai, G. (2000). Structural requirement for the two-step dimerization of human immunodeficiency virus type 1 genome. RNA *6*, 96–102.
33. Xia, T., SantaLucia, J., Jr., Burkard, M.E., Kierzek, R., Schroeder, S.J., Jiao, X., Cox, C., and Turner, D.H. (1998). Thermodynamic parameters for an expanded nearest-neighbor model for formation of RNA duplexes with Watson-Crick base pairs. Biochemistry *37*, 14719–14735.
34. Takahashi, K.-i., Baba, S., Hayashi, Y., Koyanagi, Y., Yamamoto, N., Takaku, H., and Kawai, G. (2000). NMR analysis of intra- and inter-molecular stems in the dimerization initiation site of the HIV-1 genome. J. Biochem. *127*, 681–686.
35. Gregorian, R.S., Jr., and Crothers, D.M. (1995). Determinants of RNA hairpin loop-loop complex stability. J. Mol. Biol. *248*, 968–984.
36. Klug, A. (1983). From macromolecules to biological assemblies. Angew. Chem. Int. Ed. Engl. *22*, 565–582.
37. Muriaux, D., De Rocquigny, H., Roques, B.-P., and Paoletti, J. (1996). NCp7 activates HIV-1Lai RNA dimerization by converting

a transient loop-loop complex into a stable dimer. J. Biol. Chem. *271*, 33686–33692.
38. Li, Y., and Breaker, R.R. (1999). Deoxyribozymes: new players in the ancient game of biocatalysis. Curr. Opin. Struct. Biol. *9*, 315–323.
39. Barbault, F., Huynh-Dinh, T., Paoletti, J., and Lancelot, G. (2002). A new peculiar DNA structure: NMR solution structure of a DNA kissing complex. J. Biomol. Struct. Dyn. *19*, 649–658.
40. Chen, L., and Frankel, A.D. (1994). An RNA-binding peptide from bovine immunodeficiency virus Tat protein recognizes an unusual RNA structure. Biochemistry *33*, 2708–2715.